A MFIE-Based Prediction for UHF Vertically-Polarized Wave Propagation over Irregular Terrains

Fernando J. S. Moreira
Federal University of Minas Gerais, Department of Electronic Engineering
30161-970 Belo Horizonte, MG, Brazil. fernando@eee.ufmg.br

Abstract— **A MFIE-based technique is applied on the propagation prediction of vertically polarized radio waves. The terrain profile is assumed smooth, such that back scattering is neglected and a forward scheme applied to obtain the induced surface currents. The MFIE is compared against the EFIE for several case studies. It is demonstrated that, under the present assumptions, the MFIE provides the same accuracy with a smaller number of basis functions, specially where the line-of-sight is obstructed.**

Keywords— **Electromagnetic propagation, UHF radio propagation, integral equation.**

I. Introduction

The constant expansion of wireless communication services and the associated restrictions imposed upon the radio spectrum demand accurate techniques dedicated to propagation prediction. Several works have been conducted on the use of integral equations for such predictions, due to the potentially high accuracy provided by their full-wave analysis [1]–[3]. The electric field integral equation (EFIE) was adopted by Hviid *et. al* [1] for the near-grazing incidence of a vertically polarized radio wave. The assumption of a smooth terrain profile and the neglect of back scattering enabled a forward scheme for the attainment of the induced currents, thus allowing the treatment of relatively large problems without the need of full matrices. Accelerating techniques were also presented in other studies [2],[3].

In the present work the magnetic field integral equation (MFIE) is used instead of the EFIE in cases similar to those investigated in [1]. No accelerating technique is used though. It is demonstrated that the MFIE-based technique provides the same level of accuracy with less basis functions (i.e., less segments are employed to describe the terrain profile). The advantage of the MFIE becomes specially evident for those cases were the line-of-sight (LOS) is obstructed.

II. Formulation

Due to the lack of space, the MFIE formulas will not be derived here. However the necessary steps are similar to those presented in [1] for the EFIE. Basically, a surface integral equation is employed to solve for the induced currents. For a vertical polarization, a near-grazing incidence, and neglecting any losses, the terrain is treated as a perfect magnetic conductor (PMC) and only magnetic currents are needed to satisfy the boundary conditions. The terrain is assumed smooth along the plane of incidence and perpendicular invariant. This enables the application of a stationary phase method (SPM) to solve for the integral along the perpendicular direction. The induced magnetic currents can then be obtained via the usual moment-method (MoM) matrix equation. However, by assuming a smooth profile and neglecting the back scattering, the upper-triangular portion of the impedance matrix becomes null and the magnetic currents M_n are directly obtained via a forward scheme [1]:

$$M_n \approx \frac{1}{Z_{nn}} \left(M_n^{in} - \sum_{m=1}^{n-1} Z_{nm} \, M_m \right) , \quad (1)$$

where n denotes the basis-function order and M_n^{in} is the magnetic current induced by the incident field. For the present case, these currents are oriented perpendicular to the plane of incidence. For the EFIE [1]:

$$Z_{nm} = \frac{-j\beta(\hat{n}\cdot\hat{r}_2)\sqrt{\lambda_o R_1 R_2}\Delta\ell_m e^{-j(\beta R_2 + \frac{\pi}{4})}}{4\pi R_2\sqrt{R_1 + R_2}} \quad (2)$$

for $n \neq m$ and $Z_{nn} = 1/2$ for $n = m$. Following a similar procedure for the MFIE:

$$Z_{nm} = \frac{j\beta\,\sqrt{\lambda_o R_1 R_2}\,\Delta\ell_m\, e^{-j(\beta R_2 + \frac{\pi}{4})}}{4\pi R_2\sqrt{R_1 + R_2}} \quad (3)$$

for $n \neq m$ and

$$Z_{nn} = \sqrt{\frac{2\,\Delta\ell_n}{\lambda_o}}\, e^{j\frac{\pi}{4}} \, . \quad (4)$$

Note from (2) that the term $(\hat{n}\cdot\hat{r}_2)$ indicates that the EFIE does not strongly accounts for the coupling between consecutive M_n over a smooth terrain profile.

Once the induced currents are obtained, the scattered field can be calculated as in [1]. Furthermore, the duality principle can be applied upon the previous equations for the treatment of horizontally (and, consequently, arbitrarily) polarized waves. In this case and for a near-grazing incidence, the terrain can be assumed a perfect electric conductor and only electric currents will be induced. Then, by duality, the EFIE (MFIE) for the horizontal polarization is directly obtained from the MFIE (EFIE) for the vertical polarization. In the present work only the vertical polarization is considered.

III. Case Studies

In order to verify the accuracy provided by both the EFIE- and the MFIE-based techniques, the path-loss prediction over a smooth PMC wedge was considered. The results were compared against those provided by the uniform theory of diffraction (UTD). The basic parameters are depicted in Fig. 1. The geometry is basically the one studied in [1], except that two different heights (h = 50 m and 100 m) are considered here. The dependence on the location of the receiver (d_R) was also investigated. The wedge was subdivided into several small segments, such that each segment corresponds to one pulse basis-function, as defined in [1] and adopted here likewise. Cases with 1, 3, and 5 segments per wavelength were computed at 100 MHz and 1 GHz. Both transmitter and receiver are vertically polarized infinitesimal Hertz dipoles.

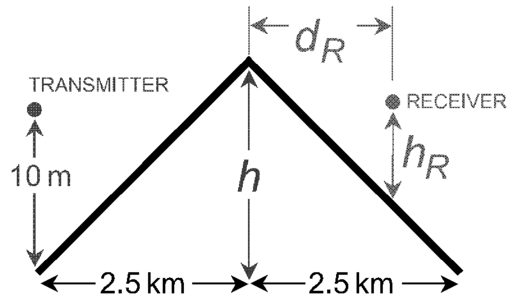

Fig. 1. The wedge geometry and basic parameters: the wedge height h, the receiver distance d_R from the wedge, and the receiver height h_R above the profile.

Initially, with d_R fixed at 2.5 km, h_R was varied from 0 up to 300 m. The numerical results for 3 segments per wavelength are shown in Fig. 2, where it is clear that the main discrepancies among the results appear inside the shadow region. The mean value (MV) of errors and the corresponding standard deviation (SD) (all with respect to the UTD results and accounting only for those points inside the shadow region) for several cases investigated are presented in Table I. From this table one initially observes that the optimum number of segments per wavelength for the EFIE is around 3 (which corresponds to the results in Fig. 2). Also, the best accuracy is obtained by the MFIE (which improves with the increase on the number of segments), except for h = 100 m at 1 GHz. For some cases, even with just 1 segment per wavelength the MFIE is capable of sustaining an appropriate accuracy.

Similar investigations were conducted, but for h_R fixed at 3 m and d_R varied from 0 to 2.5 km. The results for 3 segments per wavelength are depicted in Fig. 3, while the MV and SD for several cases are presented in Table II. The observations are basically the ones previously stated.

The comparison between the EFIE and the MFIE was further extended to the Hjørringvej profile investigated in [1]. The transmitter is placed 10 m above the profile [see Fig. 4(a)], at its beginning. The receiver is positioned 2.4 m above the profile. So, one observes from Fig. 4(a) that the LOS becomes obstructed for distances beyond 2 km. The profile was further subdivided into 0.5 segments per wavelength for each different frequency. Numerical predictions given by both the EFIE and the MFIE are depicted in Figs. 3(b), (c), and (d) at 144, 970, and 1900 MHz, respectively, where they are being compared against the EFIE-based numerical predictions presented in [1]. From these figures one observes that, even when a small number of segments is used to describe the induced currents, the MFIE still sustains the desired accuracy, specially at regions with an obstructed LOS. Furthermore, the results at 1900 MHz indicate that a larger number of segments shall be used as the frequency increases. However, the MFIE still requires less segments than the EFIE.

IV. Conclusions

This work presented a comparison between EFIE- and MFIE-based techniques for the UHF propagation prediction over smoothly irregular terrains. The results focused on a vertically polarized wave, but horizontal ones can be treated likewise by invoking the duality principle. From the cases investigated here one observes that the MFIE-based prediction yields the same level of accuracy as the EFIE one but using less basis functions to describe the induced currents, specially for those regions presenting an obstructed line-of-sight. The reduction in number of segments can come to a factor of 5 for sufficiently smooth terrain profiles. This may be explained by the fact that the mutual coupling among induced currents is not strongly accounted for by the EFIE for highly smooth profiles, where adjacent segments are almost colinear.

The results indicate the high potentiality of the MFIE-based technique for predictions over large terrain profiles, due to the tremendous reduction in computer time, even when a forward scheme is adopted to obtain the induced currents. For instance, in the forward scheme the computer time is proportional to $N(N+1)/2$, where N is the total number of segments defining the basis functions. So, the reduction in computer time is approximately proportional to N^2. Finally, accelerating techniques can also be used to speed up the whole process.

Acknowledgment

The author would like to thank Prof. J. B. Andersen for providing the data of the Hjørringvej profile and the numerical predictions presented in [1].

References

[1] J. T. Hviid, J. B. Andersen, J. Toftgård, and J. Bøjer, "Terrain-Based Propagation Model for Rural Area An Integral Equation Approach," *IEEE Trans. Antennas Propagat.*, vol. 43, pp. 41–46, Jan. 1995.

[2] C. Brennan and P. J. Cullen, "Application of the Fast Far-Field Approximation to the Computation of UHF Pathloss over Irregular Terrain," *IEEE Trans. Antennas Propagat.*, vol. 46, pp. 881 890, June 1998.

[3] C. Brennan and P. J. Cullen, "Multilevel Tabulated Interaction Method Applied to UHF Propagation over Irregular Terrain," *IEEE Trans. Antennas Propagat.*, vol. 47, pp. 1574–1578, Oct. 1999.

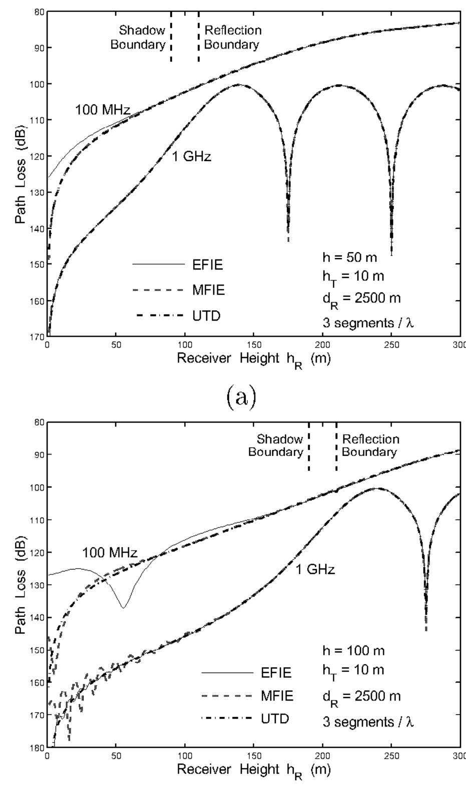

(b)

Fig. 2. Path loss prediction for the wedge as a function of h_R: a) $h = 50$ m and b) $h = 100$ m.

TABLE I

Mean-value (MV) errors and standard deviations (SD) for the path loss predictions (varying h_R) of the EFIE (E) and MFIE (M).

Frequency			100 MHz		
Segments/λ			1	3	5
$h =$ 50m	MV (dB)	E	-10.0	-2.41	-2.64
		M	-0.14	-0.12	-0.10
	SD (dB)	E	12.6	3.43	3.73
		M	0.69	0.26	0.17
$h =$ 100m	MV (dB)	E	-18.4	-1.89	-1.97
		M	-1.08	-0.17	0.04
	SD (dB)	E	13.1	6.67	7.29
		M	2.46	1.94	2.02
Frequency			1 GHz		
Segments/λ			1	3	5
$h =$ 50m	MV (dB)	E	-8.70	0.07	0.09
		M	-0.23	-0.12	-0.09
	SD (dB)	E	11.1	0.37	0.50
		M	1.04	0.47	0.31
$h =$ 100m	MV (dB)	E	-19.3	-0.05	-0.05
		M	-1.95	-0.71	-0.43
	SD (dB)	E	14.2	1.12	1.43
		M	5.57	3.36	2.57

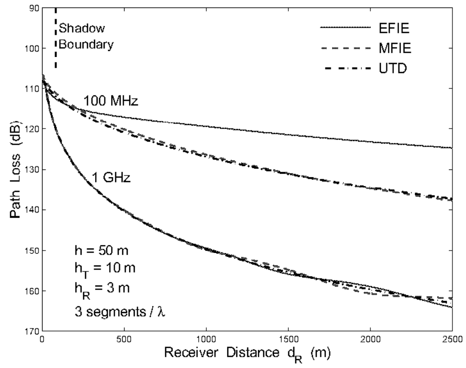

(a)

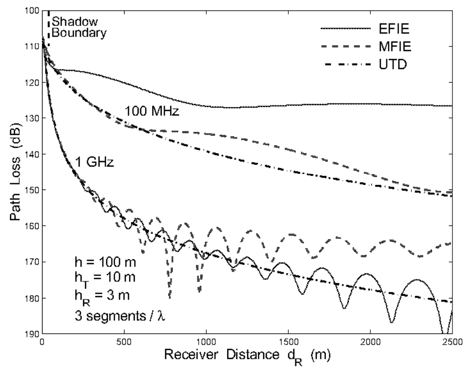

(b)

Fig. 3. Path loss prediction for the wedge as a function of d_R: a) $h = 50$ m and b) $h = 100$ m.

TABLE II
MEAN-VALUE (MV) ERRORS AND STANDARD DEVIATIONS (SD) FOR THE PATH LOSS PREDICTIONS (VARYING d_R) OF THE EFIE (E) AND MFIE (M).

Frequency			100 MHz	
Segments/λ			3	5
$h =$ 50m	MV (dB)	E	-7.85	-8.49
		M	-0.25	-0.21
	SD (dB)	E	3.66	4.05
		M	0.42	0.31
$h =$ 100m	MV (dB)	E	-15.6	-16.6
		M	-2.77	-0.44
	SD (dB)	E	6.39	6.57
		M	2.32	3.72
Frequency			1 GHz	
Segments/λ			3	5
$h =$ 50m	MV (dB)	E	0.04	0.03
		M	-0.05	-0.05
	SD (dB)	E	0.36	0.46
		M	0.51	0.32
$h =$ 100m	MV (dB)	E	0.06	0.08
		M	-6.11	-3.45
	SD (dB)	E	2.86	4.15
		M	6.04	5.11

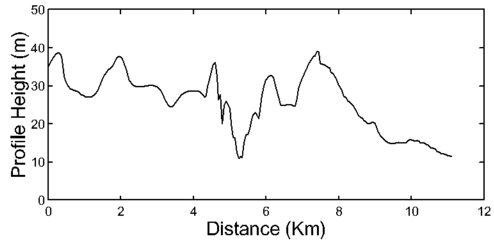

(a)

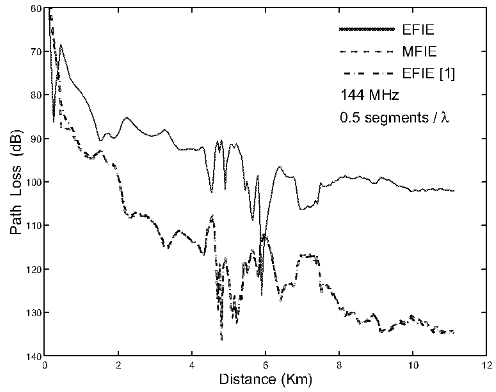

(b)

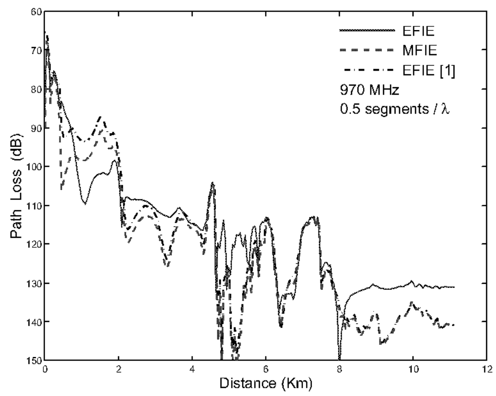

(c)

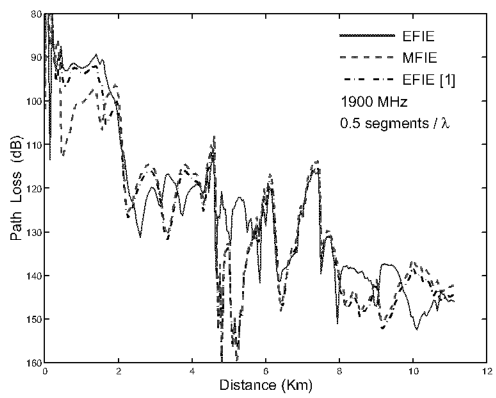

(d)

Fig. 4. Path loss predictions for "Hjørringvej" [1]: a) terrain profile and results for b) 144 MHz, c) 970 MHz, and d) 1900 MHz.